JOURNAL OF SPACECRAFT AND ROCKETS
Vol. 29, No. 1, January-February 1992

Structural Design Considerations for a Personnel Launch System

Lance B. Bush* and Christopher A. Lentz†
NASA Langley Research Center, Hampton, Virginia 23665
James C. Robinson‡
Old Dominion University Research Foundation, Norfolk, Virginia 23508
and
Ian O. MacConochie§
Lockheed Engineering & Science Company, Hampton, Virginia 23665

A vehicle capable of performing the transfer of eight people to and from the Space Station Freedom is currently in the conceptual/preliminary design stages at the NASA Langley Research Center. Structural definition of this personnel launch system and the considerations leading to it are described. Issues such as cost, technology level, human factors, and maintainability are used as guidelines for the structural definition. A synergistic design technique involving aerodynamics, performance, mission, packaging, and weights and sizing analyses is utilized to evaluate the structural design. A closed-loop design is achieved when the mission requirements are met by each previously mentioned analysis for a particular vehicle weight. Although satisfactory, the structural concept presented herein is not to be treated as a final answer, but one promising solution. An examination of alternative designs and more detailed analyses can be undertaken in order to identify design inadequacies and more efficient approaches.

Introduction

In response to a potential need to transport personnel to and from the Space Station Freedom and for assured crew return capability from the station, candidate personnel launch system (PLS) concepts are currently being designed and evaluated. Candidate configurations for the PLS include a low lift-drag ratio (L/D) biconic and a moderate L/D lifting body (Fig. 1). Initial analyses suggest that a lifting-body configuration may have advantages over other concepts because of the flexibility provided by the higher entry cross range and the low acceleration forces (1.3–1.5 g) experienced by the crew during entry.[1] Because of these aerodynamic advantages, a decision has been made to initiate a complete conceptual and preliminary design and analysis study of the lifting-body concept as an option for the personnel launch/space station rescue missions. As part of this conceptual/preliminary design effort, a candidate structural approach has been developed and analyzed. The results of this structural analysis are reported herein.

Study Guidelines

In order to conduct the configuration study, reference missions must be established. The main objectives for the PLS are to demonstrate low design and development costs and low cost per flight for a safe, reliable vehicle with efficient subsystems. Design reference missions include space station/lunar/planetary crew rotation, space station standby vehicle, and orbital rescue, sortie, and servicing. Initial operational capability is targeted for the year 2000 in order to support the Space Station Freedom. To meet the low cost goals, the configuration should incorporate current technologies or at least technologies that are projected to be available by 1992. The PLS study assumes the use of the Titan IV expendable launch vehicle and the Space Shuttle as candidate launch systems. This requirement does not preclude the use of other launch vehicles but gives a reference for vehicle weight and size for which the PLS vehicle can be designed. Key loading conditions affecting the vehicle structure are derived from the mission model. These conditions include the crew cabin pressurization, on-the-pad abort, subsonic maneuver, and runway bump. More detailed ground rules concerning the limitations and requirements of the vehicle will be introduced as needed in the remaining text.

Vehicle Design System

The design and analysis process of the lifting-body PLS candidate configuration is being conducted using a multidisciplinary approach. This approach is necessary to accurately develop a concept because the effects of each discipline impact virtually all other disciplines. This approach necessitates the simultaneous study of operations, aerodynamics, aerothermodynamics, performance, mission, packaging, structures, and weights. Through an iterative procedure, the vehicle is altered by successive discipline studies until a vehicle design meeting the vehicle weight/performance requirements is achieved. A

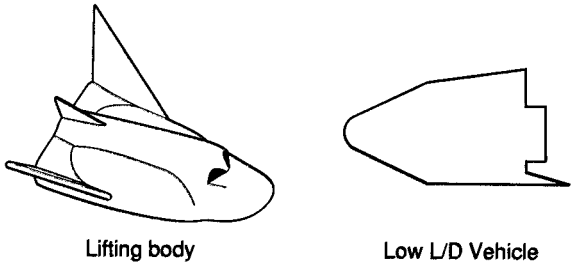

Fig. 1 Candidate personnel launch system vehicles.

Presented as Paper 90-1052 at the AIAA/ASME/ASCE/AHS/ASC 31st Structures, Structural Dynamics, and Materials Conference, Long Beach, CA, April 2–4, 1990; received April 30, 1990; revision received March 19, 1991; accepted for publication March 22, 1991.

*Aerospace Engineer, Space Systems Division. Member AIAA.
†MIT Engineering Student Coop., Space Systems. Student Member AIAA.
‡Structural Analyst. Associate Fellow AIAA.
§Staff Engineer. Associate Fellow AIAA.

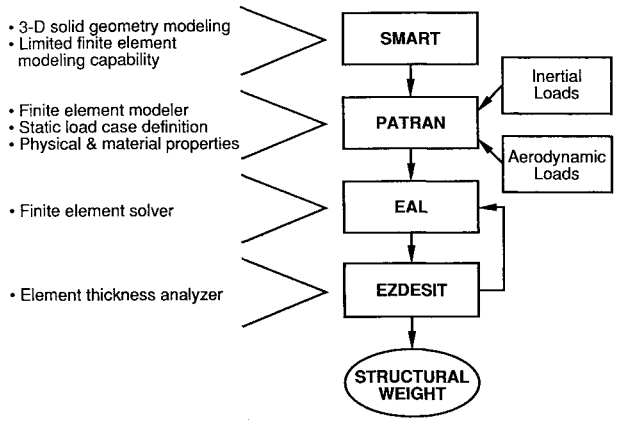

Fig. 2 Structural weights methodology.

typical iteration loop would start with the creation of the vehicle external geometry using an in-house-developed software called the Solid Modeling Aerospace Research Tool (SMART).[2] The aerodynamic characteristics of this geometry are determined through the utilization of the aerodynamic preliminary analysis system (APAS).[3] Surfaces of the vehicle geometry are then altered to improve aerodynamic characteristics. In parallel with the aerodynamics analysis, a thermal analysis of surface heating is performed using MINIVER.[4] The alterations in geometry that result from the improved aerothermal model are instituted into the original SMART geometry of the vehicle. Flight characteristics from the aerodynamic analysis and engine performance from previous propulsion studies are used as inputs to the vehicle performance analysis.

An initial vehicle weight is estimated through a combination of subsystems sizing and weight estimating relationships. The performance analysis determines the optimal trajectory and engine throttling sequence to complete the mission. In addition, the fuel fraction and gross weight of the vehicle are optimized by varying the trajectory parameters in the Program to Optimize Simulated Trajectories (POST).[5] Parallel with the aerodynamic, thermal, and performance analyses, a subsystem packaging and a vehicle structural definition are performed.

Once a tentative vehicle size has been established from the performance analysis, the vehicle structural model is sized accordingly and analyzed. The results of the structural analysis are a resized structural concept and its corresponding weight. If the vehicle weight is significantly different from the initial estimate used for performance analyses, the vehicle must be re-evaluated until the weights of both analyses converge.

Structural Design Approach

The structural analysis and weights determination includes geometry modeling, finite element modeling, loads generation and application, finite element analysis, element sizing to meet loading conditions and structural criteria, and structural element weight summation, organized into an iterating process[6] (Fig. 2). The external shape of the resulting configuration is modeled by discretizing the SMART geometry into a finite element model (FEM) through the use of PATRAN.[7] Experience is then used to initially determine and model the internal structure of the vehicle. Physical and material properties of the structure are included in the FEM of the vehicle. External loading conditions incurred during assembly, transportation, and operations are applied to the FEM. Mission static-load cases are assembled from critical POST inertial loads and APAS aerodynamic loads. The completed finite element structural model with physical and material properties,[8] external loading, and structural arrangement is ready for analysis.

The engineering analysis language (EAL)[9] is used for the finite element analysis (FEA). The FEA produces resultant structural loads due to the loading case conditions for each element. The resultant loads are indicative of the load paths of the vehicle structure. These loads are applied to the EZDESIT program[10] to size the finite elements (bars, planar beams, and plate elements) to withstand the loading conditions (Fig. 3). The cross-sectional areas of bar elements are sized. The cap cross-sectional areas and web height are sized for planar beams. The plate element design variables depend on the type of construction chosen. Isotropic and composite honeycomb, hat-stiffened, and membrane panels along with corrugated web elements can be sized by the code. For each element, a stiffness matrix and a construction geometry (lamina gauge, honeycomb core height, etc.) are specified, and each element has an initial thickness equal to the minimum gauge value. The elements are sequentially checked for failure due to panel buckling, stability criteria, yield, and ultimate modes for each loading case. If failure occurs, the element dimensions are increased until the indicated failure mode is satisfied. The geometric sizing of the panel alters the stiffness properties. Thus, the finite element analysis and geometry sizing are iterated until convergence is achieved.

The dominant failure load case for each element is determined, and its corresponding dimensions, weight, and failure mode are obtained. The results of the sizing can be reviewed in two different manners. An interactive session of the EZDESIT program permits the user to write the results to the terminal screen. The resulting weight of the vehicle structure is calculated and displayed by component, load case, failure mode, and element type. In the second method, the EZDESIT output file is read into PATRAN, and the element properties can be displayed on the model. Those properties include internal loads, dominant load case, failure modes, and unit weights. Highly stressed areas may indicate a need for an alternative structural design. Resultant loads are reviewed by the structural designer, and the necessary changes to the structural arrangement are made by altering the FEM and reanalyzing the structure.

Vehicle Definition

Initial studies of using the lifting-body concept as a PLS result in a baseline vehicle length of 24.56 ft. The Space Shuttle payload bay diameter is a factor limiting the PLS size, particularly its span. The Titan IV limits the maximum weight of the PLS and adds complexity to the structural arrangement of the PLS due to aft end mounting. Since the space station is visualized as having an eight-member crew, the PLS vehicle should have room for 10 people, that is, a pilot, copilot, and eight passengers. The external surfaces serve as walls for the pressurized crew compartment to maximize the personnel headroom. Entry and exit hatches are necessary for entrance to and exit from the PLS vehicle while on the launch pad, during docking to the space station, and in the event of an emergency water landing evacuation. The hatch located on the

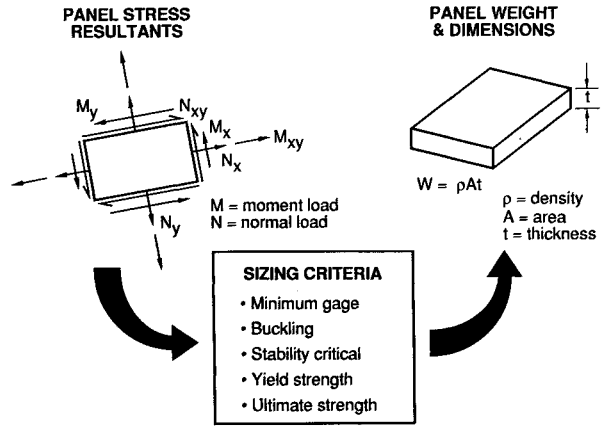

Fig. 3 Element sizing methodology.

top of the vehicle can be used for prelaunch access and in case of a water landing for egress. The aft hatch is primarily for use in docking with the space station. In addition, enough internal volume must be available for the retractable landing gear, orbital maneuvering system (OMS), reaction control system, prime power, environmental control and life support system, avionics systems, and personnel provisions. The internal packaging arrangement is shown in Fig. 4.

The baseline vehicle length of 24.56 ft was increased photographically to a length of 26.52 ft. At this new size, the vehicle still fits into the Space Shuttle payload bay and is within the Titan IV's launch capability. The need to analyze various vehicle sizes stems from the as yet unsolved internal volume needs. Both sizes of the vehicle have been analyzed to obtain a vehicle sizing relation. The analysis and results of the smaller (baseline) vehicle (24.56 ft) will be discussed in this paper, and results of the larger (26.52 ft) vehicle will be presented as a sizing comparison.

Structural Definition

When defining the structure of the PLS, several points must be considered, such as the vehicle configuration, subsystems arrangement, mission scenarios, cost, and maintainability. The various sections of the vehicle will be designed to accommodate various design criteria.[11] Aerodynamic loading may be the major design criterion for the wings, whereas internal pressure and volume requirements may be the driving criteria for the crew compartment. Engineering judgement was required to identify criteria and their corresponding structure for many of the subsystems.

The proposed structural concept (Fig. 5) for the vehicle body shell and fins contains current technology materials and construction with the exception of a new approach for the thermal protection system (TPS) attachment. The vehicle shell will have either internal skin stringer or internal isogrid stiffeners. Frames, also internal to the skin, will be located approximately every 20 in. This distance is subject to change with further optimization or changes in vehicle size. The stiffeners and frames are internally placed so as not to interfere with carrier panels and the TPS. The carrier panels are multipurpose. Supporting the TPS on a carrier panel, rather than a skin, reduces the chances of TPS loss from structure flexing. The carrier panel additionally provides more space between the TPS with its high entry heating and the vehicle skin. The carrier panels will be constructed of a lightweight composite material, probably a graphite/polyimide. The carrier panels are used only on the bottom surface of the crew compartment area. Direct application of the TPS is used on the remaining surface areas of the vehicle. Even though the thermal protection system is similar to that now used on the Space Shuttle, more testing and design will be necessary because of the carrier panel addition. High-density reusable surface insulation (HRSI) is employed on the bottom surface of the vehicle and low-density reusable surface insulation (LRSI) and/or flexible reusable surface insulation (FRSI) on the upper surfaces (Fig.

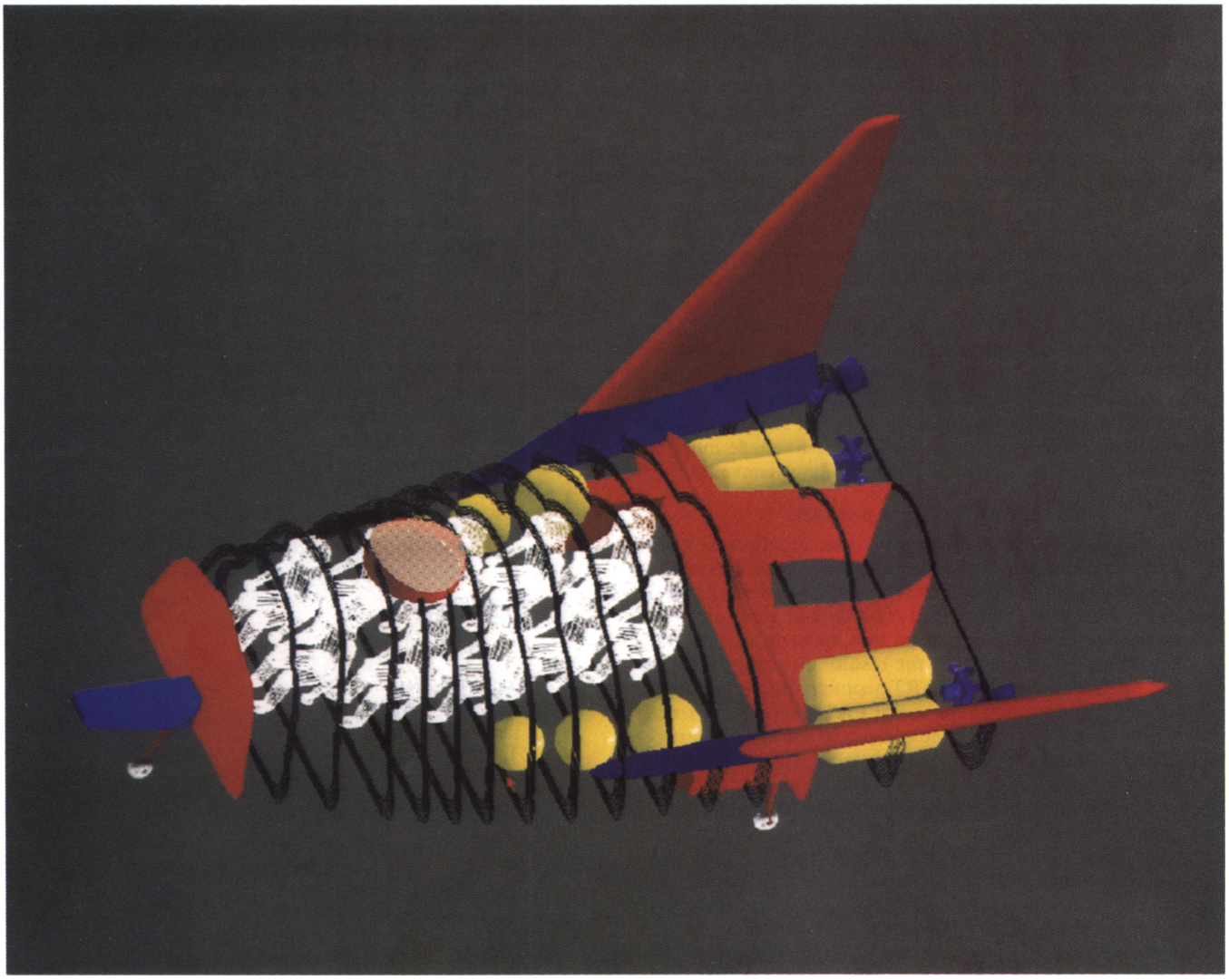

Fig. 4 PLS internal arrangement.

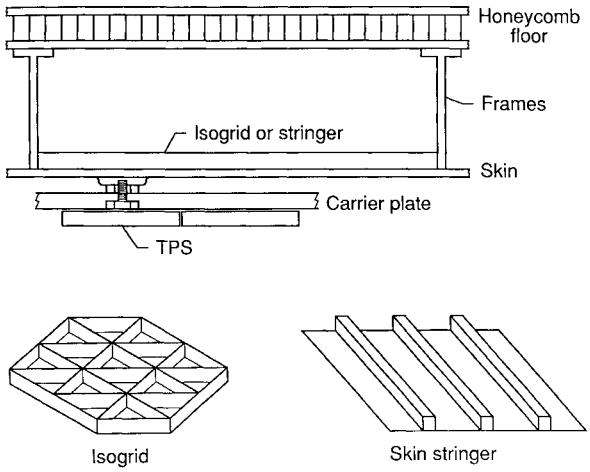

Fig. 5 Proposed PLS structural concept.

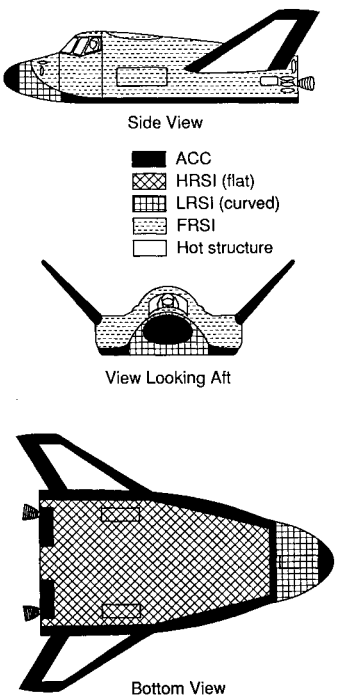

Fig. 6 PLS thermal protection system.

6). Advanced carbon-carbon (ACC) is used in areas of high heating such as on the wing leading edge and control surface, nose, chines, and vehicle body flaps.

Aluminum (2219) is used for the crew cabin pressurized shell because of its low cost, high-use experience, and its weldability. The crew cabin is welded to insure sealing of the pressurized vessel. Within the crew compartment, a honeycomb floor will be mounted on the primary ring frames. The honeycomb will consist of Kevlar skins and a Nomex core. Subsystems will be secured to the structure at the frame locations. Aluminum (7075) will be used as the construction material for the forebody thereby reducing weight because of its higher strength. Much of the forebody will consist of a molded ACC nose cap similar in construction and installation to the Space Shuttle's nose cap. The construction of the aft body will be similar to that of the crew compartment with the omission of the floor and carrier panels. Composite boron aluminum tubular struts will be used for the OMS engine thrust structure and tank supports. These same struts will be used in several other locations on the vehicle to support subsystems, provide a tensile or compressive load path, and reduce shell deflections under internal pressure.

Other significant structural components, besides the ring frames, must be included in the internal arrangement of the vehicle. A forward and an aft bulkhead will complete the crew compartment. Larger ring frames in the aft section of the vehicle serve to stiffen the body as well as provide a load path for the wing-spar-to-body intersection. In addition, points along the ring frames will be used to attach the OMS subsystem. Four large axial beams serve as seat tracks and transmit the combined inertial load of personnel, suits, and seats to the OMS propulsion or abort rockets at the rear of the vehicle. These axial beams will also reduce vehicle flexure. Ribs and spars are placed in the wing to provide load paths into the body.

Vehicle Model

A FEM representing the previously described vehicle structure was created. This model includes elements that represent structure, materials, and physical properties. Several materials are utilized in the design of the vehicle. These material properties are input as tables in the finite element modeling program and are assigned to corresponding elements composed of a

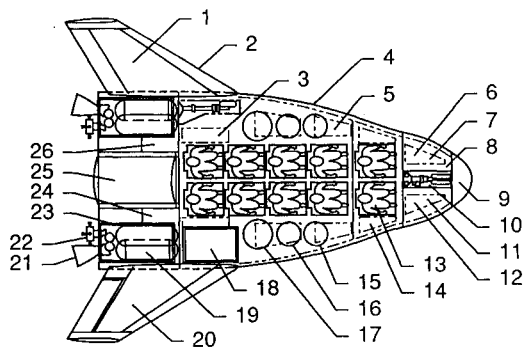

Subsystem	Weight, lb
1 Wing	260
2 Leading edge	40
3 Environmental control life support subsystem	150
4 Mid body	1325
5 Environmental control life support subsystem	150
6 Environmental control life support subsystem	63
7 Forebody	42
8 Reaction control system	40
9 Nose cap	47
10 Nose gear	47
11 Evaporator H_2O	480
12 Avionics	200
13 Personnel, suits, + seats (per)	417
14 Avionics, displays, + controls misc.	300
15 Cabin N_2 & tank	89
16 Cabin & fuel cell O_2 + tank	259
17 Fuel cell H_2 + tank	123
18 Landing gear main	230
19 Orbital maneuvering system	1580
20 Surface control	25
21 Orbital maneuvering system	24
22 Reaction control system	60
23 Surface control	25
24 Avionics	200
25 Tail	26
26 Aft body	650

Fig. 7 PLS subsystem packaging and weights.

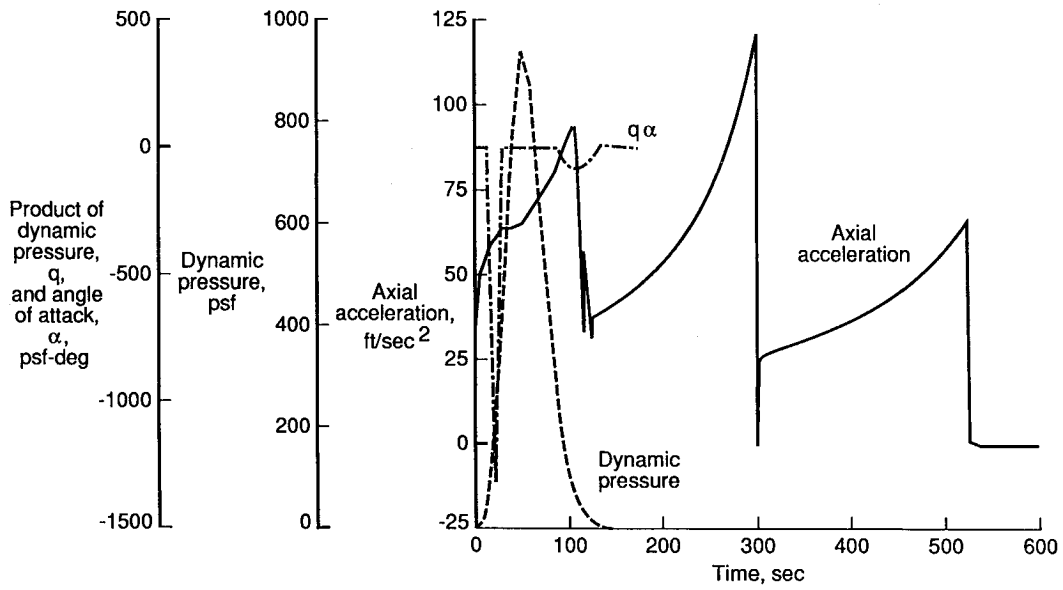

Fig. 8 POST Titan IV ascent performance.

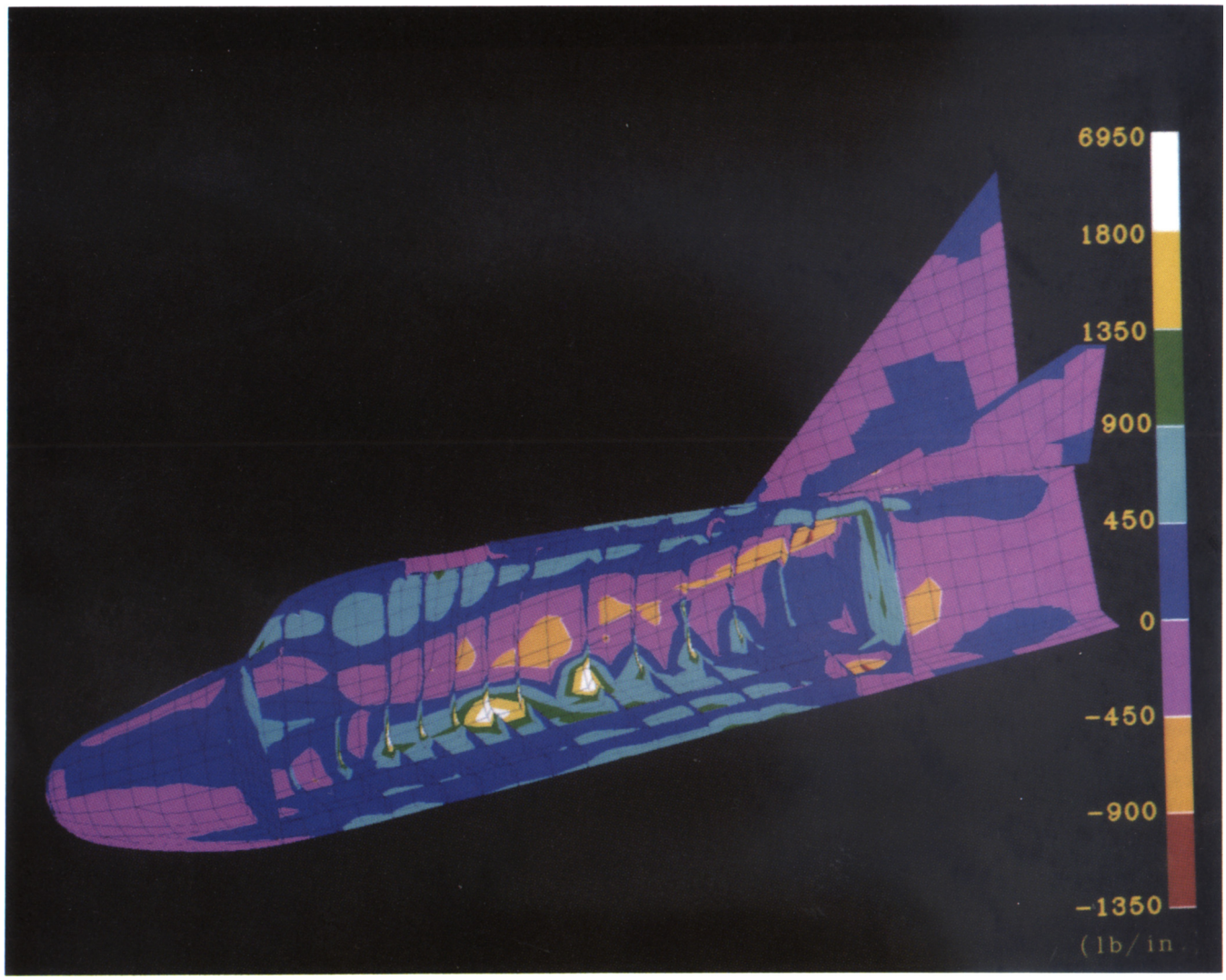

Fig. 9 Resultant lateral body loads due to on-orbit cabin pressurization.

specific construction material. Geometric properties were also tabulated and assigned to corresponding elements to model the stiffness of the various types of construction methods. That is, the stiffness properties of a membrane and an isogrid construction differ and these properties are needed to calculate the resultant stress levels due to loading. Most of the vehicle structure is modeled using the physical properties of a skin stringer construction. Bulkheads are modeled using plate properties with bar stiffeners. Ring frames are modeled using membrane properties for webs and bar properties for the caps. Ribs and spar webs are modeled assuming membrane properties. All physical properties are initialized as manufacturing minimum gauge. Through sizing loops, these gauges will be increased as needed to prevent failure or remain minimum gauge in cases of negligible loading.

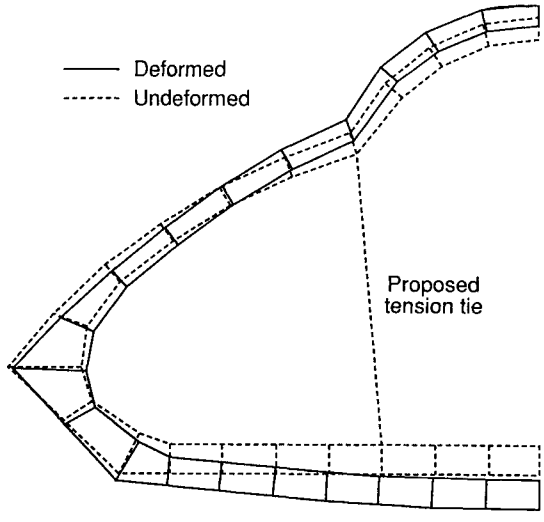

Fig. 10 Vehicle cross sectional deflection due to on-orbit cabin pressurization.

Elements representing the subsystem masses are also included in the FEM. These nonstructural elements are important because they introduce inertial forces into the structure when coupled with vehicle accelerations. Masses of the subsystems (i.e., avionics, fuel tanks, etc.) are calculated using weights and sizing routines. The calculated subsystem masses are influenced by technology level and cost. These masses are placed on the structure consistent with the subsystem packaging arrangement in Fig. 7. In the case of personnel provisions, masses need to be calculated for the personnel, pressure suits, and seats. In accordance with the study guidelines, each of the crewmen is assumed to be a 95th percentile white male. This is a worst-case scenario since some personnel on each flight will probably be of lesser stature. According to Ref. 12, a 95th percentile white male corresponds to a weight of 217 lb. A partial pressure suit weight for each person is 86 lb. Initial weight estimates are 114 lb per seat, giving a total of 417 lb for each suited crewman in his seat.

Vehicle Loads

Once the geometry, material, and mass modeling of the vehicle are completed, external loading conditions for the PLS

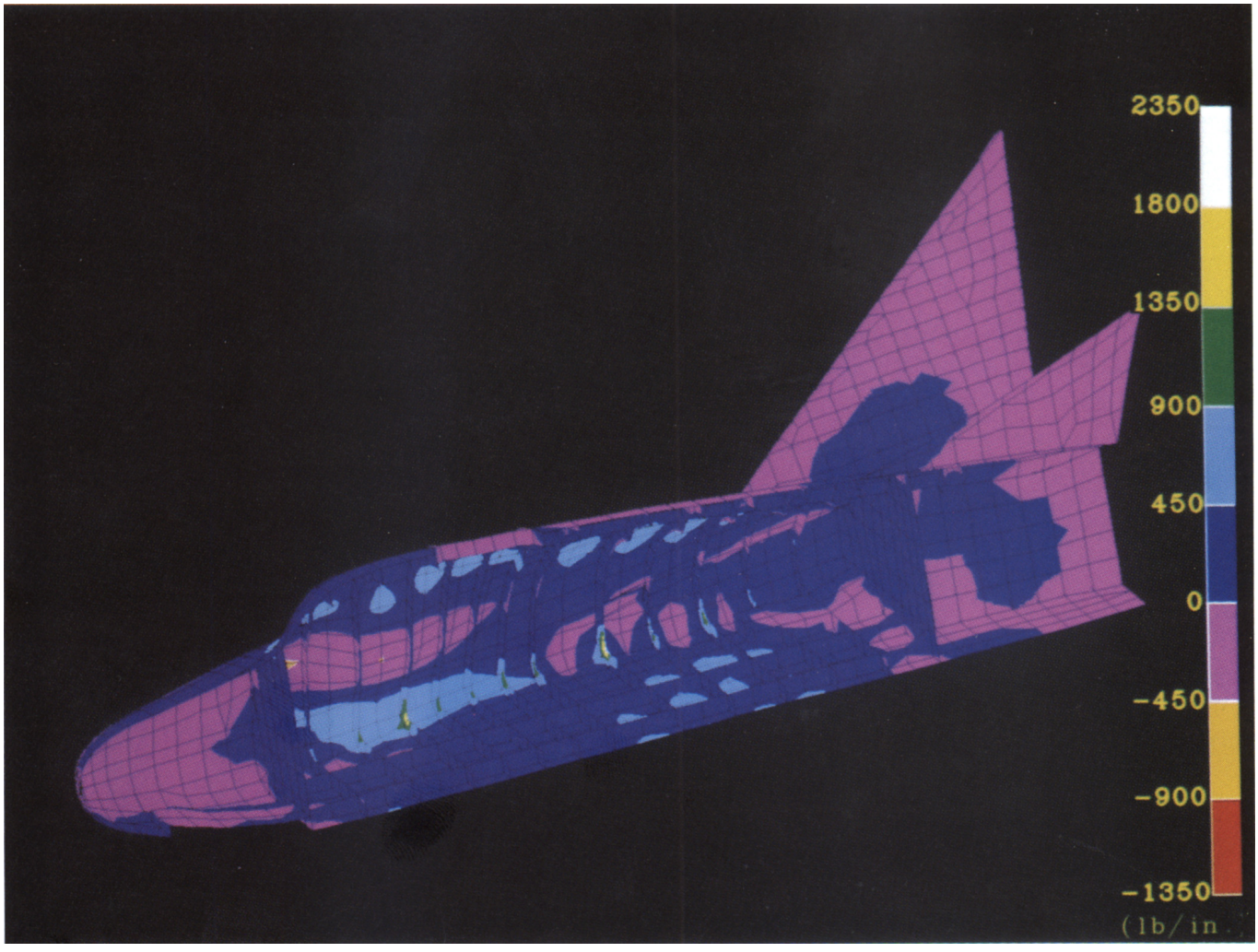

Fig. 11 Resultant lateral body loads (with tension ties) due to on-orbit cabin pressurization.

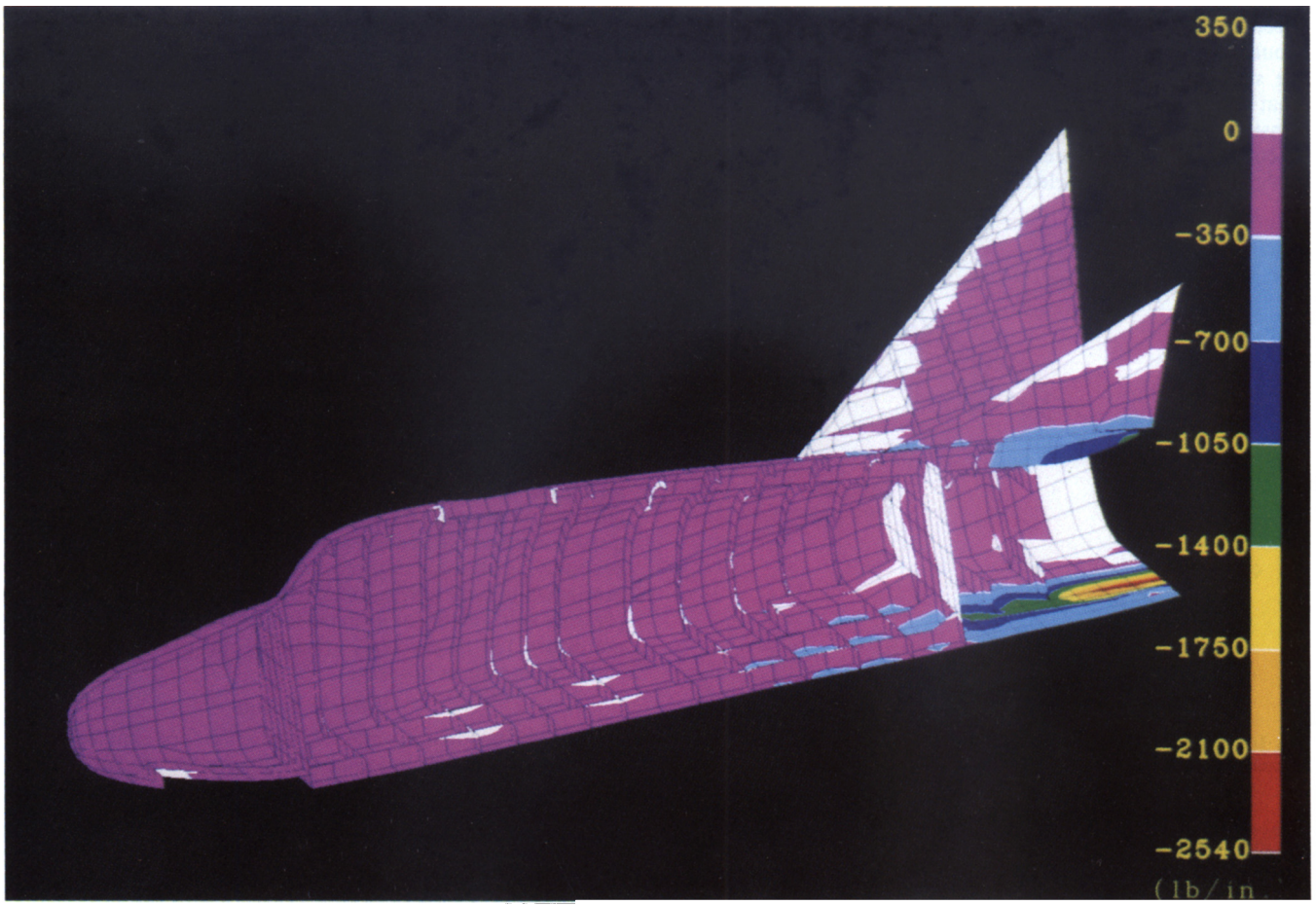

Fig. 12 Resultant axial thrust structure loads due to on-the-pad abort.

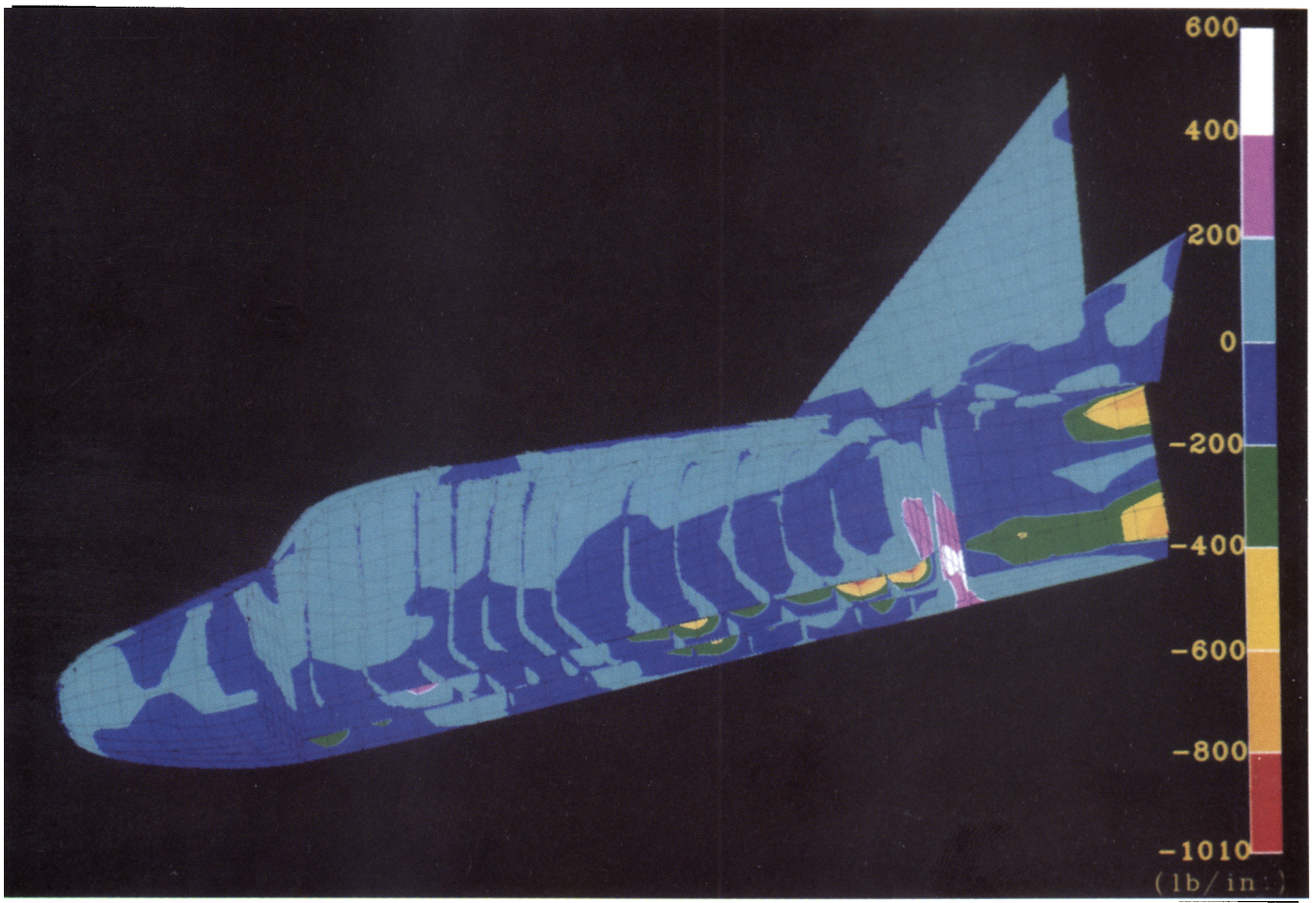

Fig. 13 Resultant axial body loads due to on-the-pad abort.

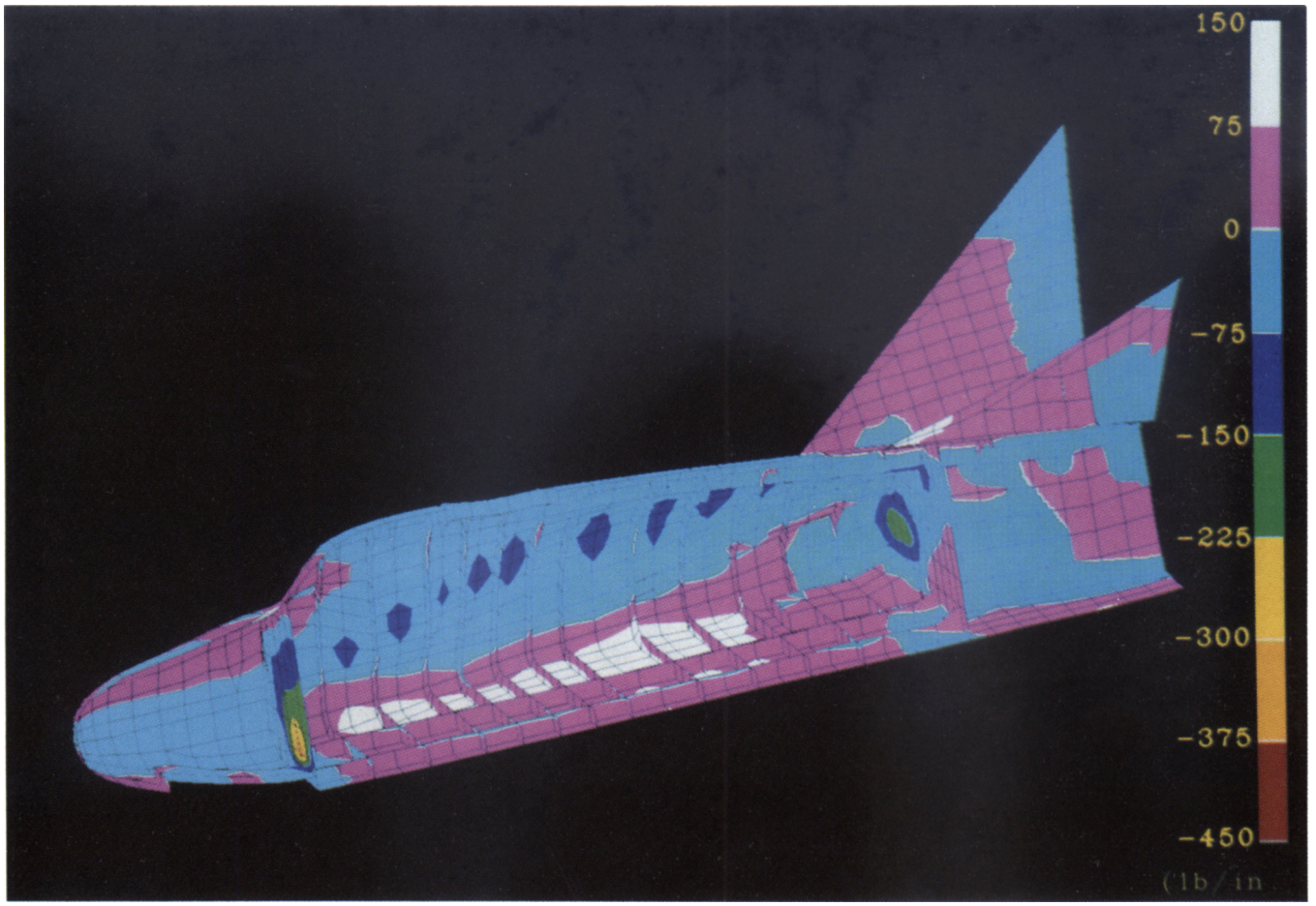

Fig. 14 Resultant axial body loads and normal bulkhead loads due to a runaway landing bump.

Fig. 15 Resultant axial body loads and spanwise wing loads due to subsonic aerodynamic maneuver.

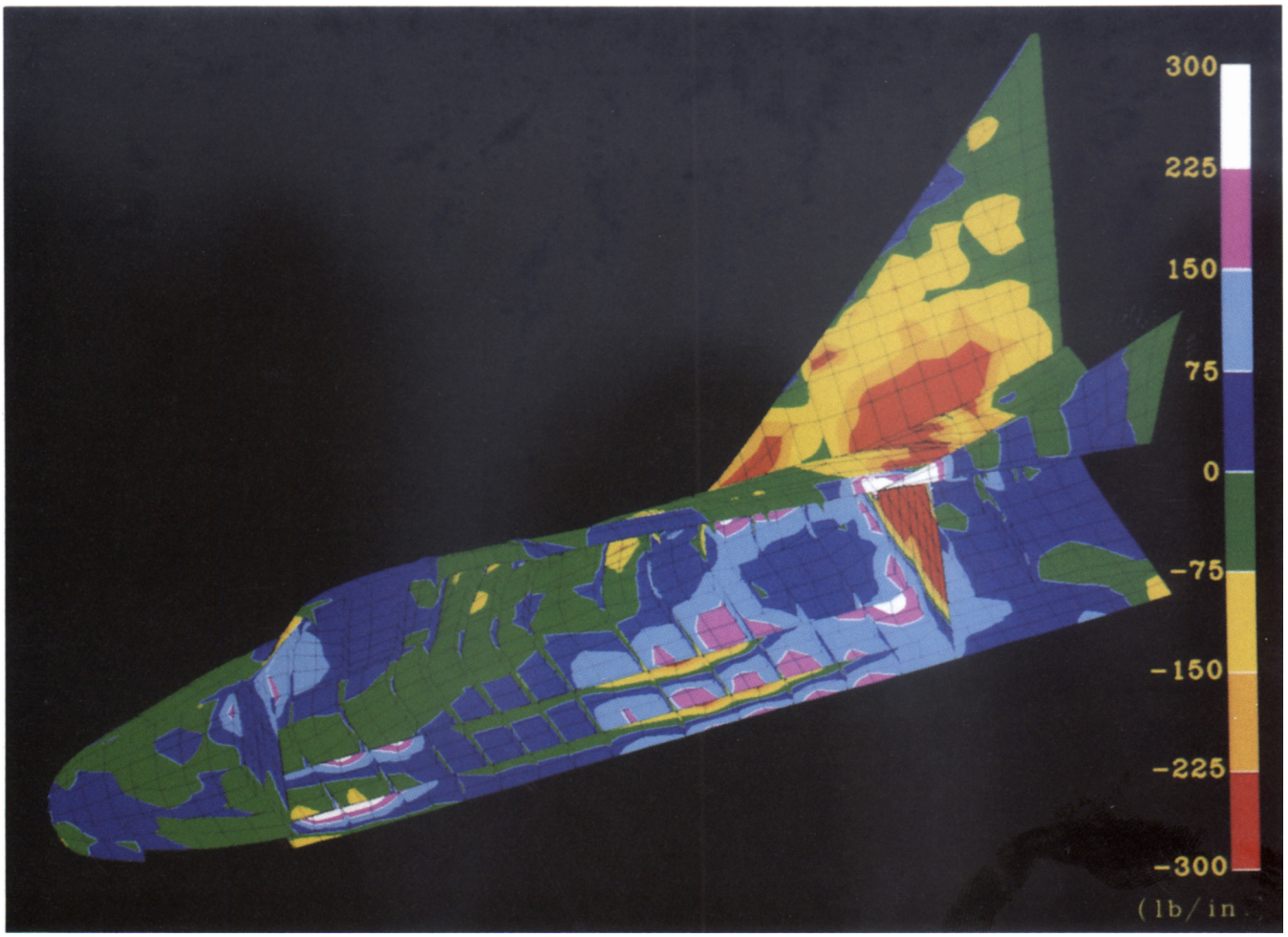

Fig. 16 Resultant lateral body loads and chordwise wing loads due to subsonic aerodynamic maneuver.

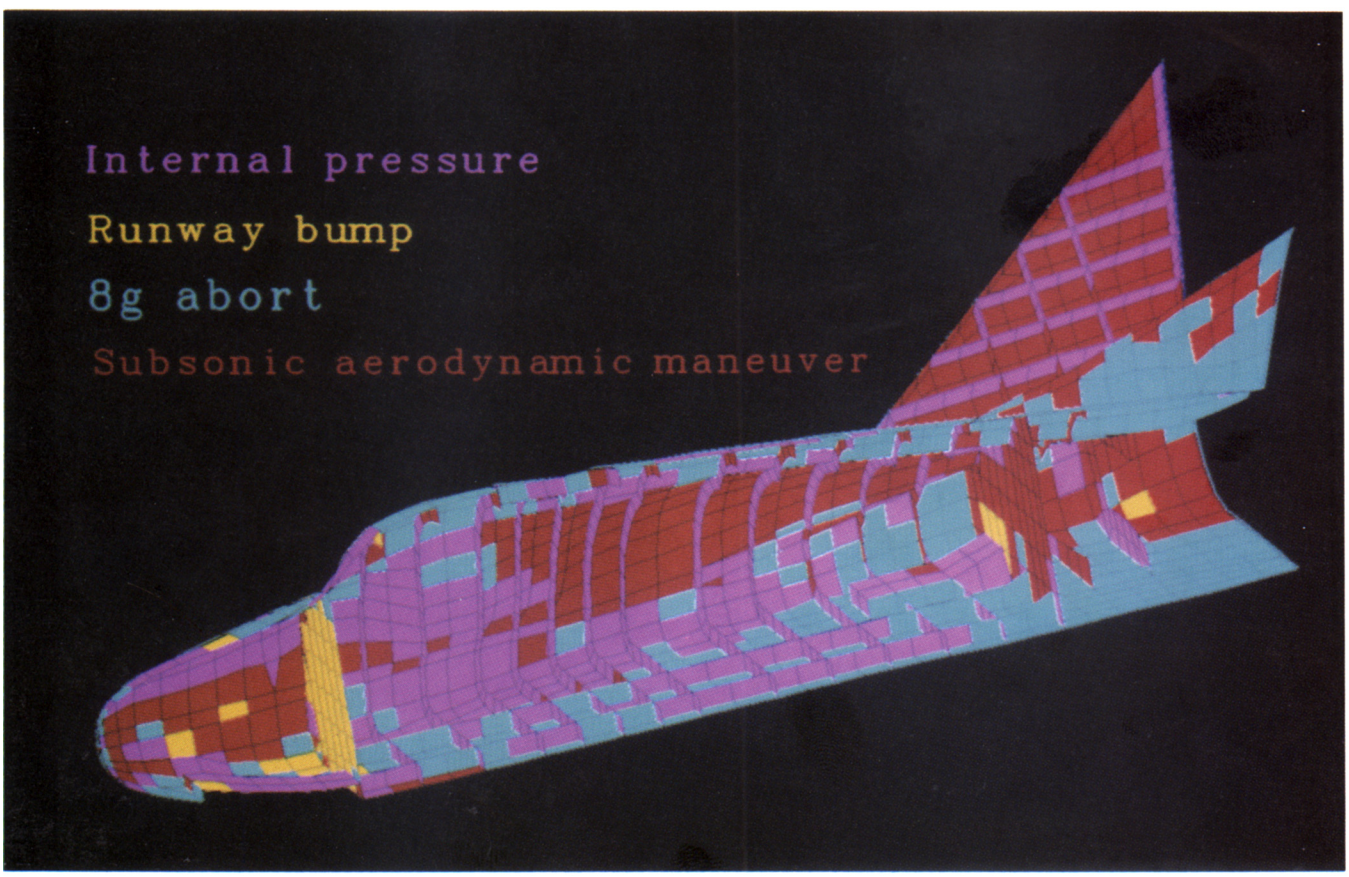

Fig. 17 Dominant panel sizing load case.

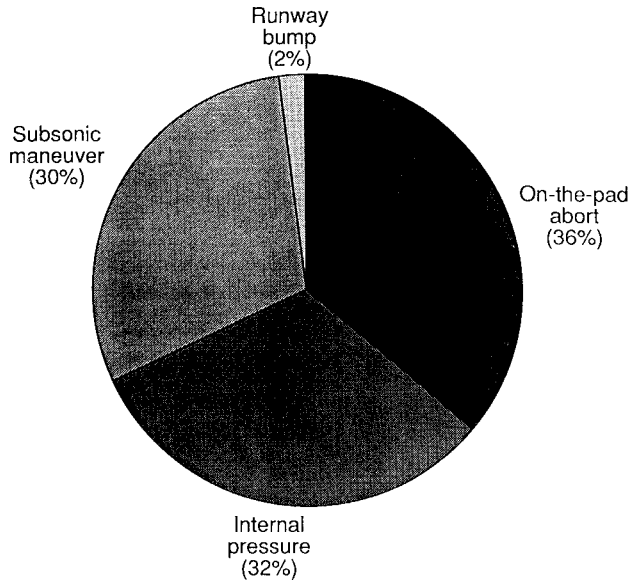

Fig. 18 Vehicle structural weight by load case.

are defined. An examination of the operations and mission of the vehicle should result in design loading conditions. These conditions occur when loads are maximum for a specific area or component of the vehicle. For example, the wing is expected to experience its maximum loading after atmospheric re-entry and during subsonic maneuvers. Loading during ground operations is typically much less than that experienced during the mission. Thus, a description of the mission and its sequences starting with the launch phase is necessary to obtain the maximum loading conditions.

The primary mission is the transport of personnel to Space Station Freedom, or other orbital nodes, and return to Earth. The PLS may function in other capacities consistent with the primary capability, such as on-orbit servicing and orbital transfer to other space nodes. From the standpoint of structural design, all missions will typically include launch, ascent, orbit, docking, berthing, deorbit, descent, and landing loads. The spacecraft structure must also sustain loads for all phases of an abort, including pad or altitude aborts at high dynamic pressures.

An on-the-pad abort yields a critical loading condition. In order to escape an explosion and its resulting overpressures, an 8-*g* acceleration (*g* is the acceleration due to gravity, 32.2 ft/s^2) must be accomplished by the PLS module through the use of its abort motors mounted on the interface adaptor. This axial acceleration is the maximum experienced by the vehicle in a normal mission or abort. At launch, all of the fuel and cargo are onboard, yielding the maximum inertially induced forces on the vehicle. This condition is modeled by applying constraints at the interface adaptor/PLS attachment bolts, whereas the vehicle FEM and its associated subsystem masses are subjected to inertial loads equivalent to an 8-*g* forward acceleration. Once the vehicle is jettisoned away from the blast and over the ocean east of Kennedy Space Center (KSC), parachutes are deployed and a water landing is accomplished. Water impact loads could reach levels as high as 10 *g* due to combined effects of the vehicle deceleration and wave action. In the event of an on-the-pad abort into the water, the vehicle must remain intact to insure survival of the crew, but intact survival of all of the structure outside the pressure shell is not a requirement. Parachutes are stored in the adapter and are positioned and deployed so that the aft end of the vehicle enters the water first. This entry allows for a lower deceleration at water impact. Several precautions are taken to ensure the safety of the personnel. The vehicle will not be analyzed for water impact since this is an allowed failure and the aft structure should not be designed to withstand these loads without failure. However, the structure is to be designed so as not to deform to the extent that it would jeopardize the integrity of the pressure shell.

A performance analysis of the vehicle ascent using POST (Fig. 8) does not result in any higher axial loading than is sensed during the abort mode. Although there are normal and axial loads present during ascent, their summation is relatively insignificant compared with abort loads. Furthermore, the vehicle's structural arrangement is such that most of the load paths are either axial or lateral, with little interaction between them. Engineering codes are unable to accurately predict the aerodynamic pressures due to sideslip rotations or gust loads. This may be of little importance since the gust velocities are significantly smaller than the vehicle velocity and rotations during launch will be overpowered by the launch vehicle propulsion and control system.

During the later stages of ascent, external aerodynamic and inertial loads are relatively small. Yet, one of the design loading conditions occurs during this time. Environment compatability with the Space Station Freedom is specified as one of the ground rules for this study. Thus, the crew compartment is designed for a 14.7-psi internal pressure. This absolute pressure at sea level becomes a 14.7-psi differential at altitude across the crew compartment shell and constitutes one of the critical design conditions. The pressure differential is typically not a major concern when dealing with cylindrical or spherical tank-like structures, but the crew compartment has one flat side and three curved surfaces with differing radii of curvature. The internal pressure over the flat floor is approximately 1 ton/ft^2, or approximately 270,000 lb. This condition was modeled by applying a 14.7-psi pressure to the interior face of each element comprising the crew compartment.

No significant vehicle loads occur during docking or berthing. Some local loading will occur, but this constitutes an insignificantly small contribution to structural weight compared with other loading conditions.

Upon re-entry, aerodynamic effects become significant on the vehicle. The vehicle flies at an angle-of-attack range from 27 deg at hypersonic entry conditions to 2 deg at low supersonic speeds. The maximum dynamic pressure during this phase of entry occurs around Mach 2.5 where the flight angle of attack is 6 deg. At this condition, pressures on the wing are in the neighborhood of 3 psi. The aerodynamic pressure exerted on the body is insignificant in comparison with the already mentioned internal pressure. A subsonic maneuver of 2.5 *g* normal to the vehicle floor is assumed. The vehicle acceleration and aerodynamic pressure values result from APAS and POST analyses. A load case is simulated on the FEM by placing the corresponding aerodynamic pressures on the model along with inertial forces equivalent to the 2.5-*g* normal acceleration on the FEM and its subsystem masses.

A maximum landing sink rate of 3 ft/s is assumed. Performance analyses show that this sink rate is achievable for all touchdown scenarios with a margin of 1 ft/s included for a worst case. A touchdown deceleration at a sink rate of 3 ft/s results in only a 0.35-*g* acceleration normal to the vehicle. This value is based on a gear stroke length of 5 in. A portion of any short-term landing accelerations are attenuated by the seats. Conventional design landing loads usually include a 2.5-*g* runway bump condition. This condition will be used since its loads exceed those for the touchdown. This will be modeled by placing inertial forces equivalent to the 2.5-*g* normal acceleration on the FEM and its subsystem masses and restraining the landing gear body attachment points.

Additional loading cases will be added in the future as deemed necessary by more analysis. At the writing of this paper, more aerodynamic analysis and wind-tunnel testing are in progress and more detailed performance analyses are underway. The results of the additional research and testing will be included in future structural analyses of the PLS configuration.

Finite Element Analyses Results

Internal loads caused by the aforementioned applied loading conditions are calculated from FEA using EAL. These resultant loads can be displayed on the vehicle model using PATRAN. Visual inspection of element local lateral and axial resultant loads is used to determine areas of the vehicle or components in need of an alternative structural design. Load levels of high magnitude may be indicative of a poor initial structural design. A discussion of the FEA results and modifications follows.

Initial analysis of the on-orbit internal pressure loading case indicates that a large portion of the crew compartment structure is subjected to relatively high load levels (Fig. 9). Top and bottom skins of the crew compartment are loaded in transverse tension, and the midsection is in compression. A look at the cross-sectional deflection under the assigned loading condition explains this difference in resultant loads (Fig. 10). The internal pressure acting on the longer horizontal span exerts enough force to deflect the top and bottom surfaces outward, with the maximum deflection occurring at the centerline. The shorter span in the vertical direction causes compression in the fuselage skin due to the reversal in frame bending moments. After this initial analysis, a solution to reduce the deflections and load levels was proposed in the form of tension ties. Tension ties are placed in the crew compartment, connecting the inner flanges of the frames. Keeping these stiffeners outboard of the personnel seats maintains the seating volume and egress paths. As a result of this new structural arrangement, the level of the resultant loads and deflections due to internal pressure were reduced (Fig. 11). This reduction in load level resulted in a structural weight savings of 576 lb, based on a structure sizing failure analysis.

Results of the on-the-pad abort analysis show the loading to be localized to the aft end of the vehicle (Fig. 12). Axial running loads in the sides of the thrust structure have a maximum value of 1000 lb/in. at the top and bottom skin intersection points. These loads dissipate quickly and are essentially noncritical before they approach the aft bulkhead of the crew compartment. This is because the aft bulkhead, which is perpendicular to the thrust structure, does not provide for a good load path. In contrast, axial running loads reach a maximum of 2450 lb/in. in compression in the skins of the top and bottom surfaces (Fig. 13). These loads do not dissipate below 700 lb/in. until well into the back third of the crew compartment. The bulkhead does contribute to a reduction in the axial loads in the skins as seen at their junction. Loads at the aft end are reduced by a factor of 3 within a very short lateral distance from the thrust structure. Thus, additional longitudinal stiffeners may decrease the resultant stress levels. Compression at each bolt attachment is assumed. If a yawing action were to occur during flight (not analyzed herein), the compression at some bolt locations would be reduced, perhaps enough to cause tension, whereas the compression load at some locations would increase to produce a critical load case. As mentioned earlier, performance analyses are being conducted to assess the probability of this occurring. If this scenario is found to be probable, the case will be analyzed.

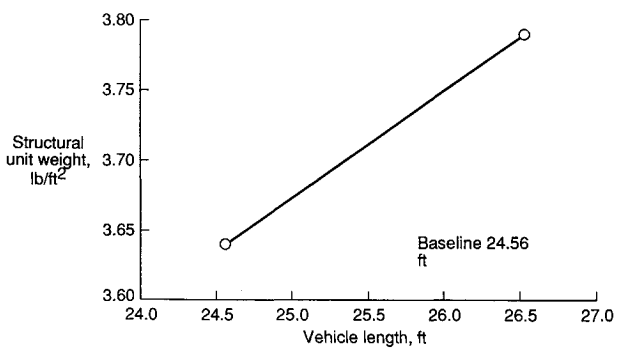

Fig. 19 Vehicle structural unit weight sizing relation.

The results of the runway landing conditions show localized loads at the landing gear bays and more specifically in the bulkheads to which the main strut of each gear is attached (Fig. 14). The direct impact of this type of loading is contained within the bulkheads and dissipates quickly. Indirectly, the vehicle flexes from the impact, resulting in tensile loads for the bottom and compressive loads for the top of the vehicle within the crew compartment area. These loads switch location in the nose as this acts as a cantilevered beam with no support at the forward end. The overall effect of these loads on the vehicle will probably be negligible because of their low magnitude compared with those already seen in the cases of abort and internal pressure. One area that will be affected by this loading is the bulkheads since they take a load that is applied within their planes. Additional bulkhead stiffeners may be necessary to withstand these loads and reduce the stresses.

The subsonic maneuver analysis results exhibit the effects of the aerodynamic wing loading and the 2.5-*g* normal acceleration on the entire vehicle (Figs. 15 and 16). As expected, the lower surface of the wing is in tension and the upper surface of the wing is in compression, as noted by the respectively positive and negative load values. These loads tend to cluster at the leading edge because of the shorter load paths into the body structure. Exact dimensions of the trailing-edge control surface have not yet been determined, but the lack of loads in this area indicates this to be a minor adjustment. A comparative study of the load cases shows the wing resultant loads to be greatest for this loading condition. A combination of the wing loads entering the body and the normal acceleration on the body creates the resultant body load map.

Similar to the wing loads, the body experiences axial tension in the lower surface and axial compression in the upper surface. The unusual intersection angle of the wing and body introduces a canted load path in the body. These paths can be critical because of the abrupt change of curvatures found on the body surface. The axial loads are mainly due to the normal acceleration flexing of the structure (Fig. 15). Lateral loads in the body are also in tension on the bottom surface and in compression on the top surface (Fig. 16). In contrast to the axial loads, these lateral loads are additionally induced by the introduction of wing loads into the body. Aerodynamic loads deflect the wing upward, placing a moment load at the wing/body intersection. This moment is evident in the lateral loads of the body. The wing deflection places a compressive load into the upper skin and a tensile load into the lower skin. The ring frames and the bulkhead of the body act to carry the load through the body, as exhibited in the high load levels. Thus, the wing and parts of the body may be critically loaded by the subsonic aerodynamic maneuver.

Resultant loads discussed in the previous text are used as input to a structural sizing failure analysis. Certain physical properties of each element are sized to withstand an array of structural failure criteria. The exact details of this operation are found in the Structural Design Approach section of this paper. A weight for each sized element results from this sizing operation. The critical condition for an individual panel can be determined and displayed (Fig. 17). A review of the failure case loading picture shows good correlation with the results of the individual load case scenarios.

The subsonic aerodynamic maneuver sizes the wing and upper body sections. The upper body section was in compression due to the normal acceleration and the wing deflection of this scenario. Loads running into the aft bulkhead due to the wing bending account for the sizing of the bulkhead by this condition. The sizing of the lower portion of the nose is also attributed to the subsonic aerodynamic maneuver. The nose is cantilevered from the forward bulkhead and incurs compressive loads in this region.

The on-the-pad abort sizes most of the upper and lower surfaces of the aft end of the vehicle. The abort loading is not

localized to the aft end as was noted in the discussion addressing that topic. Much of the resultant loads act through the plane of the lower surface and upper surface. The load is not reduced significantly until well into the crew cabin. Thus, the large in-plane loads acting on the floor cause the panels to be sized by that criterion rather than the loads due to pressurization or aerodynamic maneuvers.

The condition affecting the least amount of the structure is the runway bump. Figure 17 exhibits the localized loading experienced by the bulkheads because of this loading condition. This condition introduced loads directly into the plane of the bulkheads. Resultant loads for the aft bulkhead were small compared with the other scenarios, and only the section of the bulkhead directly in contact with the landing gear is sized by this condition. The forward bulkhead experienced direct in-plane loading only for the runway bump scenario. Thus, the forward bulkhead was sized almost entirely by the runway bump conditions.

As suspected, the internal pressure loading has a significant impact on the sizing of the vehicle. The deflection of the crew compartment because of this loading contributed to the large loads in the skins of the vehicle and the seat tracks. Although some of the floor is sized by the abort scenario and some of the top skins are sized by the subsonic maneuver, the remaining structure is sized by the internal pressure.

The vehicle structural weights required for the various design conditions are presented in Fig. 18. If one case were to dominate the sizing of the vehicle, consideration would be given to modifying that mission scenario. Results indicate that the vehicle is not designed disproportionately for any one case. In fact, the resulting weight is almost evenly split among the three major loading conditions. The runway bump condition is a localized loading condition and therefore does not have a large effect on the entire vehicle.

The EZDESIT program is used to calculate the weight and unit weight of each resultant element based on its corresponding sized structural and material properties. The resulting vehicle weight agrees with that obtained through the other discipline studies, making this a converged concept. An average unit weight of 3.64 lb/ft^2 was calculated for the entire vehicle primary structure. The larger vehicle (26.52 ft) also attained convergence. The weight of the vehicle increased by approximately 700 lb for a new unit weight value of 3.79 lb/ft^2. No significant scaling of any one subsystem in comparison with the rest was noted. A graphical representation of the vehicle unit weights vs length exhibits the weight sizing relation of the vehicle (Fig. 19). This approach can also be utilized to represent the sizing relationship for each subsystem. The sizing relationships resulting from the analyses enhance the weights and sizing data base. Future adjustments of the vehicle size can be accomplished with more ease, utilizing the relationships calculated by this method.

Studies of the PLS are continuing. Results reported in this paper should be regarded as a progress report and not a final report. Exact size of the vehicle is undetermined as yet and may increase. If needed, additional analyses will be performed. The maximum size will be limited by the chosen launch vehicle. A few more structural tradeoff studies will be performed, as noted previously. Many of these studies will center around the body location of structural members and slight improvements of the material properties. Major alternative structural arrangements and subsystem packaging for the vehicle are being examined and will be analyzed as required.

Summary and Concluding Remarks

A lifting-body vehicle design has been proposed for the purpose of transporting personnel to and from the Space Station Freedom. This PLS is currently in the conceptual/preliminary design phase. The PLS structural design reported within this study is capable of performing the assigned mission within the limits of the prescribed guidelines for vehicles within a length range of 25–27 ft. No limiting structural technologies have been identified for these vehicles. This study is continuing in an effort to determine the optimum vehicle design and to identify and solve any possible structural design problems.

References

[1]Ware, G. M., Spencer, B., and Micol, J. R., "Aerodynamic Characteristics of Proposed Assured Crew Return Capability (ACRC) Configurations," AIAA Paper 89-2172, July 1989.

[2]McMillan, M. L., Rehder, J. J., Wilhite, A. W., Schwing, J. L., and Mills, J. C., "A Solid Modeler for Aerospace Vehicle Preliminary Design," AIAA Paper 87-2901, Sept. 1987.

[3]Cruz, C. I., and Wilhite, A. W., "Prediction of High-Speed Aerodynamic Characteristics Using the Aerodynamic Preliminary Analysis System (APAS)," AIAA Paper 89-2173, July 1989.

[4]Engel, C. D., and Praharaj, S. C., "MINIVER Upgrade for the AVID System. Volume I: Lanmin User's Manual," NASA CR-172212, Aug. 1983.

[5]Brauer, G. L., Cornick, D. E., Olson, D. W., Petersen, F. M., and Stevenson, R., "Program to Optimize simulated Trajectories (POST), Vol. II," Martin Marietta Corp., MCR-87-583, Denver, CO, Sept. 1987.

[6]Bush, L. B., Lentz, C. A., Rehder, J. J., Naftel, J. C., and Cerro, J. A., "Structural Weights Analysis of Advanced Aerospace Vehicles Using Finite Element Analysis," AIAA Paper 89-2130, July 1989.

[7]Anon., "PATRAN Plus User's Manual," Release 2.3 Pub. 2191020, PDA Engineering, Costa Mesa, CA, July 1988.

[8]Anon., "Materials Engineering/Materials Selector 1988," Penton, Cleveland, OH, 1987, pp. 71,190.

[9]Whetstone, W. D., "Engineering Analysis Language Reference Manual," EISI, San Jose, CA, July 1983.

[10]Cerro, J. A., and Shore, C. P., "EZDESIT, A Computer Program for Structural Element Sizing and Vehicle Weight Prediction," NASA TM-101649, 1990.

[11]Anon., "Structural Design Criteria Applicable to a Space Shuttle," NASA SP-8057, Jan. 1971.

[12]Anon., "Man-Systems Integration Standards," Vol. 1, NASA STD-3000, March 1987.

Earl A. Thornton
Associate Editor